Desalination and Water Treatment
www.deswater.com
doi: 10.1080/19443994.2013.791767

51 (2013) 6961–6969
November

Taylor & Francis
Taylor & Francis Group

Optimization-based periodic forcing of RO desalination process for improved performance

M. Al-haj Ali, A. Ajbar, Emad Ali*, K. Alhumaizi

Department of Chemical Engineering, King Saud University, PO Box 800, Riyadh, 11421, Saudi Arabia
Tel. +96 614678650; Fax: +96 614678770; email: amkamal@ksu.edu.sa

Received 5 March 2011; Accepted 27 February 2013

ABSTRACT

The performance of a tubular reverse osmosis (RO) process for water desalination is investigated using periodically forced feed parameters. The study was performed using a dynamic model that was developed and validated in a previous work. Simultaneous forcing of feed pressure and flow rate were studied. Fully symmetric rectangular pulses were used for input forcing because of their applicability for digital control implementation. It was found that the simultaneous periodic operation of the RO inputs improves its performance in the sense of higher permeate flow rate and reduced salt concentration. Increasing the pressure forcing amplitude will further enhance the performance; however, the attainable performance is limited by the constraints on the operating pressure. Depending on the RO unit constraints and characteristics, a maximum increase in permeate flow rate up to 42% and reduction in salt concentration of about 20% could be obtained.

Keywords: Reverse osmosis; Cyclic operation; Symmetric forcing function; Water desalination

1. Introduction

Reverse osmosis (RO) process is an important filtration process that is used extensively for the desalination of sea and brackish water all over the world. Concentration polarization and membrane fouling are the major problems faced in the any membrane-based separation operation. The ultimate effect of these factors is to reduce the permeate flux and consequently loss of productivity. Fouling effects are characterized, in some cases, by an irreversible decrease in flux. In real practice, severe fouling may require shutting the process down for cleaning the membrane by chemical or physical methods. Concentration polarization on the other hand results in reversible decline in water flux through the membrane. Usually, concentration polarization can be controlled via two main methods [1]: (i) changes in the characteristics of the membrane [1] and (ii) modification of flow rates and flow regime. The latter requires introducing instabilities in the flow of the RO process [2,3]. Examples of such approach includes backwashing and periodic operation of the module, through forcing some of the process variables [4]. Periodic forcing improves the mixing of the solution on the feed side and, hence, reduces the build-up of solute ions near the membrane wall. The analysis of periodically forced RO has received considerable attention in the literature. One of the first works in this area was carried out by Kennedy and coworkers [5] who varied harmonically the flow rate of sucrose

*Corresponding author.

solution in an RO unit. For a frequency of 1 Hz, the authors reported an enhancement in the permeation flow rate by 70% over the corresponding steady-state operation. Ilias and Govind [6] followed the experimental work in [5] and developed a mathematical model to evaluate the unsteady-state operation of tubular membranes through changing the inlet feed flow harmonically. They concluded that flow pulsation offered an alternative, cost-effective method to improve the transmembrane flux. Al-Bastaki and Abbas [4] modified the model that was proposed by Kennedy and coworkers [5] so that it can be used for asymmetric square waves. The authors, further, studied the effect of using an asymmetric pressure square wave on the performance of an RO process. They found that cyclic operation lead to an increase in the permeate flux of about 6.5% over that obtained from steady-state operation. The increase in performance was attributed to the reduction in concentration polarization in the process. The same authors [7] used a simple model to predict the performance of periodically forced RO system. Abbas and Al-Bastaki [8] also studied the periodic performance of a seawater desalination unit based on a small-scale commercial spiral wound membrane. For the case of unsteady-state operation, the operating pressure was varied according to a symmetric square wave function around an average pressure of 50 bar. The production rate increased as the period of the wave decreased. Such an improvement was obtained at the expense of a marginal increase in the total energy consumed. Abufayed [9], on the other hand, reported the experience from the periodic operation of the Tajoura seawater RO plant in Libya. Different methods used to enhance membranes performance were also reviewed by Al-Bastaki and Abbas [10]. Ali et al. [11] studied the performance of an RO tubular membrane module under oscillatory feed pressure conditions using a validated rigorous dynamic model [12].

In the earlier work [11], the RO performance in terms of enhanced permeate production was examined by periodic forcing of a single input which is the feed pressure. Only the effect of the frequency of the periodic function is examined. No rigorous optimization was considered to optimize the forcing periodic function. In this study, we extend the work of Ali et al. [11] to investigate the simultaneous forcing of two inputs, namely the feed pressure and flow rate. Furthermore, the forcing function will be designed using rigorous optimization tools. Exclusively, symmetric cyclic functions will be investigated to ensure that performance improvement is due to periodic forcing and not because of changes in the input steady-state value.

2. Process model

The cycling study is based on a dynamic model of tubular membranes that was developed and validated in an earlier study [12]. Both steady-state and dynamic behavior were validated against a laboratory-scale experimental unit. The model considers the unit as a series of single tubes with appropriate minor pressure losses introduced between them. Each tube is described by coupled differential algebraic equations. The tubes are modeled and solved sequentially where the output of any tube becomes the input for next tube. Model equations are summarized in the appendix. The feed condition of the model is set to feed pressure of 35 bar, feed velocity of 38 cm/s, and salt concentration of 2000 ppm. When the RO is operating at steady state, the quality of the product is set to permeate flow rate of 0.36 cm^3/s, and salt concentration of 108.2 g/l.

2.1. Forcing variables

For cyclic operation, two shapes of forcing functions have been employed in published works, namely sinusoidal inputs and square wave variations [13]. In this study, square wave variation is considered as shown in Fig. 1. Rectangular pulses are more suitable for discrete control application as it is easier to program and implement. Only symmetric shape of the pulses will be investigated. By symmetric, it is meant that the periodic function will oscillate up and down around the mean with exactly the same magnitude, that is, amplitude. Moreover, symmetry implies the pulse width is exactly half of the period. In this case, the mean of the periodic function equals to the steady-state value of the process input as shown in Fig. 1. This is to guarantee that the process

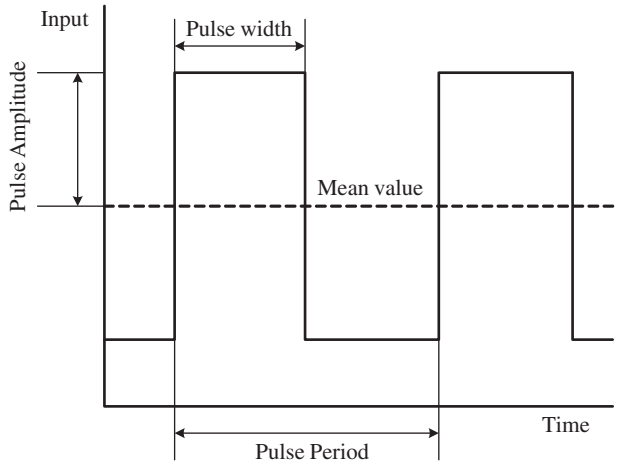

Fig. 1. Schematic diagram of a symmetric pulse.

performance enhancement is due to cyclic operation rather than changes in the steady-state value of the input. Symmetric pulse shape is characterized by two parameters: pulse amplitude and pulse period. But being symmetric, the pulse width is equal to half the pulse period. Therefore, the forcing parameters to be investigated are the pulse amplitude and pulse period for both inputs, that is, the feed pressure and velocity. Design of the forcing parameters will be determined by solving the following optimization problem:

$$\max_{A_{m1},A_{m2},P_w} \Phi = w_1\bar{q} + w_2\frac{1}{\overline{C_p}} + w_3P_w \quad (1)$$

Subject to:

$$\dot{x} = f(x,u) \quad (2)$$

$$\begin{aligned} P_w^L &\leqslant P_w \leqslant P_w^U \\ A_{m1}^L &\leqslant A_{m1} \leqslant A_{m1}^u \\ A_{m2}^L &\leqslant A_{m2} \leqslant A_{m2}^u \end{aligned} \quad (3)$$

In the equations above, A_{m1} and A_{m2} are the pulse amplitude of the first and second input, which are the feed pressure and velocity, respectively. P_w is the pulse width for both inputs, $\bar{q}$ is the average value of the permeate flow, and $\overline{C_p}$ is the average value of the permeate salt concentration. Moreover, w_1, w_2, and w_3 are weights on the optimized variable. The purpose of these weights is to differentiate between the importance of their corresponding variables. The higher the weight, the more important is the optimized variable. The average values of q and C_p are obtained by averaging their dynamic response over a specific simulation time. The dynamic responses are obtained by solving the dynamic Eq. (2) which represents the RO model given in the appendix. The dynamic model is solved for a given periodic input function. The optimization problem is solved subject to the constraints on the design parameters A_{m1}, A_{m2}, and P_w.

The optimization solution is carried out using sequential approach. The optimization solver sets the values of the pulse characteristics from which the rectangular pulses are composed and sent to the dynamic model solver. The model is then simulated over a specific simulation time using rigorous numerical integration routine. The results are averaged and sent back to the optimization solver. The procedure is repeated till convergence is approached. The entire procedure is handled by MATLAB (version 5.3) software. In particular, the routine *fsolve* and *ode23* are used to solve the differential algebraic equations and *fmincon* is used to solve the optimization problem. The convergence criterion of the optimization solver is fixed by the parameters of the *fmincon* routine.

It should be noted that when the optimization problem is solved a unified simulation interval of 10 time units is used for all cases for fair comparison and to ensure that the process has reached a steady-state behavior. Depending on the value of P_w, the number of input cycles within the simulation interval may vary. Thereof, the numerical solution methodology is programmed such that exact integer multiple of a single pulse period is used within the specified simulation interval. The purpose is to avoid bias in the average value of the input function, and consequently, the average value of the process key variables, that is, q and C_p.

3. Results and discussion

First, the optimization problem is solved for fixed pulse width of 20 sampling instants. The pulse width is the same for both input cyclic functions. The results are listed in the first row of Table 1. It should be emphasized here that P_w is kept fixed and was excluded in Eq. (1) as design variable. The bound on the design parameters was set to $2 \leqslant A_{m1} \leqslant 30$ and $2 \leqslant A_{m2} \leqslant 30$. The optimal values of the pulse amplitude are ± 30 bar for the feed pressure and ± 21.755 cm/s for the feed velocity. Note that the pulses amplitudes are in change from the corresponding steady-state values of the inputs. In this case, the steady states are 35 bar and 38 cm/s for the feed pressure and flow rate, respectively. The RO dynamic response that corresponds to the optimal periodic function is depicted in Fig. 2. It is clear that the cyclic operation of the feed pressure and flow rate resulted in a transient behavior of the RO system to new values. The average value of the permeate flow is 39.3% higher than that when the process operates at steady feed pressure of 35 bar and steady feed velocity of 38 cm/s. The average value of the salt in concentration in permeate is 19% lower than that when the process operates at steady state.

Next, the optimal value for the pulse parameters, that is, A_{m1}, A_{m2}, and P_w are optimized by solving Eq. (1) for the same bounds on the pulse amplitude

Table 1
Optimization results

w	P_w	q/q_{ss}	C_p/C_{pss}	P_f (bar)	u_f (cm/s)
1,1	20	1.393	0.810	30	21.755
1,1,0	82	1.414	0.803	30	21.669
1,1,1	91	1.397	0.804	30	20.576
1,1,10	299	1.419	0.914	30	27.082

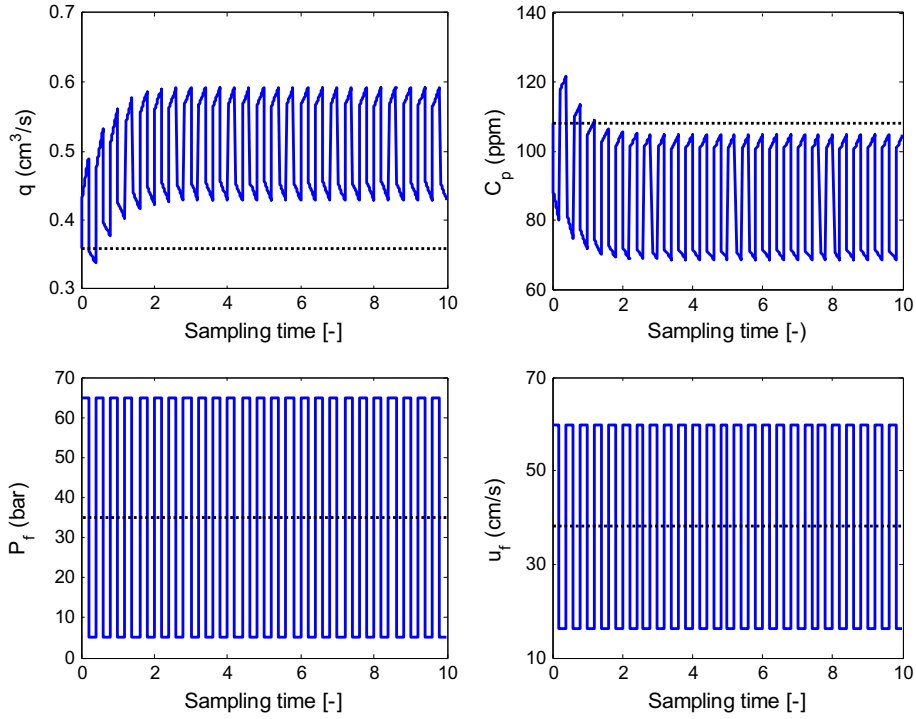

Fig. 2. Process variables response operating at periodic function with optimal amplitude and fixed pulse width, dashed: steady state, solid: process variable.

and additional bounds on the pulse width of 1 and 300. It should be noted that the pulse width is unified for both input periodic functions. The results are illustrated in Table 1 starting from row 2 to the end. The second row of Table 1 shows the results when the pulse width was not maximized by being excluded in the objective function, that is, $w_3 = 0$. It should be noted that setting $w_3 = 0$ does not exclude P_w from being used as a design variable to optimize Eq. (1). In this case, the optimal pulse parameters are ± 30 bar for the change in feed pressure amplitude, ±21.669 cm/s for the change in feed velocity amplitude and 82 samples for the pulse width. Applying the input pulses with these optimal specifications into the process resulted in performance improvement manifested by 41.4% increase in the permeate flow and 19.7% decrease in the salt concentration. It can be seen that the process performance is improved over what was obtained at fixed P_w, although the obtained pulse amplitudes have almost the same value at fixed P_w. This proves that the pulse width has impact on the effectiveness of the input function on the process performance. It is desirable from real practice to increase the pulse width to avoid high frequency of input fluctuation. For this reason, maximization of the pulse width is included in the objective function by increase its corresponding weight, that is, w_3. The outcome for this case of $w_3 = 1$ gives higher value for P_w with minor loss of the permeate flow rate. When more weight is given to maximizing P_w by increasing w_3 to 10, the optimization solution moved toward maximum value of pulse width of 299 sampling unit while maintaining excellent enhancement in permeate flow rate. However, the salt concentration in the product deteriorates. The obtained results are still acceptable as it provides reasonable performance which cannot be obtained when operating the process at steady input values.

For further investigation of the pulse width effectiveness, additional simulations were conducted. Fig. 3, for example, demonstrates how the average value of permeate flow and salt concentration vary with the pulse width at fixed value for the pulse amplitude. In due course, the amplitude change from steady state is fixed at the optimal values of ± 30 bar and ± 21.75 cm/s. For each pulse width, a periodic input function is generated using the designated pulse width and the fixed amplitudes. The model is numerically integrated using the devised input from which the average value for q and C_p is obtained. Repeating the process for different values of P_w, the curves in Fig. 3 are generated. In fact, the curves depict the ratio of the average permeate flow to the static value (q/q_{ss}) and ratio of the average value of the salt concentration

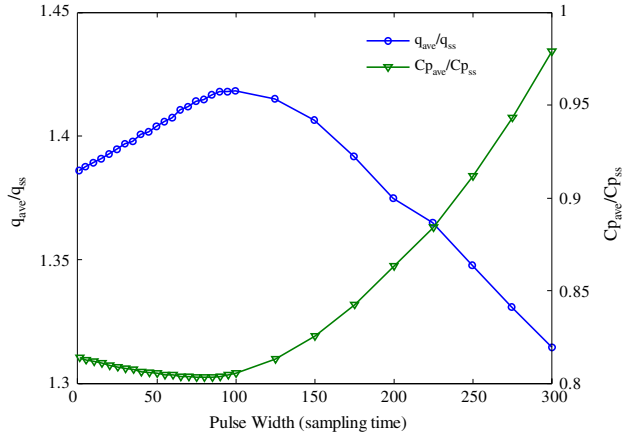

Fig. 3. Effect of the pulse width on the process performance at fixed pulse amplitudes.

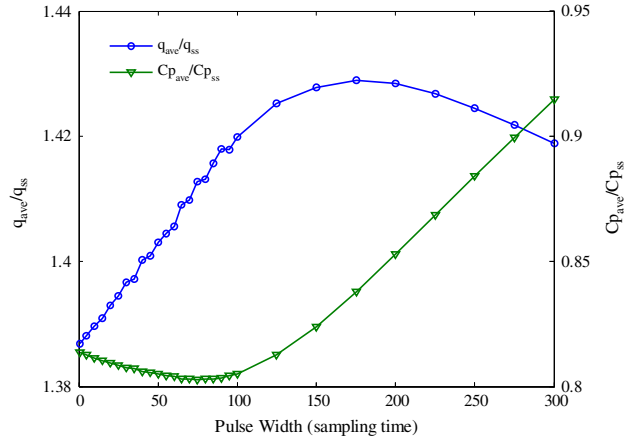

Fig. 4. Effect of pulse width on the process performance at optimal pulse amplitudes.

to the static value (C_p/C_{pss}). It can be observed form the figure that permeate flow increases with P_w till it reaches a maximum around P_w of 100 sampling unit then decreases rapidly. Similar behavior is detected for the salt concentration but in the opposite direction. Moreover, the minimum occurs at P_w of 75 sampling unit.

For more rigorous analysis, the previous tests are repeated without fixing the pulse amplitude. The consequence is illustrated in Fig. 4. Here, at each pulse width, the optimization problem Eq. (1) is solved to obtain optimal values for the pulse amplitudes. Consequently, the obtained average values for the process variables are plotted. Obviously, similar trend to that in Fig. 3 is revealed. However, two distinctions can be detected. First, the improvement in permeate flow occurs at wider range than that for fixed pulse amplitudes. The distant between location at which maximum q occurs and that at which minimum C_p occurs becomes wider a part. Therefore, it is hard to find a unified pulse width that satisfies both performance requirements. It should be noted that different pulse amplitude can be obtained at each P_w because the optimization is revisited for each case. For this reason, a sample of these results is listed in Table 2 to demonstrate how pulse amplitude may vary from case to case. It is clear that the optimum pulse amplitude for the feed pressure always occurs at its upper bound. For the feed velocity, the optimum pulse amplitude remains close to a value of 22 cm/s except at very high pulse periods. It should be noted that the permeate production in Figs. 3 and 4 is not a smooth function due to numerical round off error.

The results of Table 2 indicated the effectiveness of the upper bound on the feed pressure as in all cases the optimum solution was at the allowable upper limit. For this reason, the impact of the upper limit on the feed pressure is analyzed. To allow for larger upper values, the initial value for the feed pressure (the mean value around which the pressure oscillates) should be increased above 35 bar. Figs. 5 and 6 illustrate the optimization results, when the initial feed pressure (P_{ss}) is set to 45 bar and the permissible upper limit (Δp^u) of the pulse amplitude change is set to three different values at 20, 30, and 40 bar. For comparison purposes, the figures include the result when the initial pressure is fixed at 35 bar and the upper limit on the pulse amplitude is fixed at 30 bar which exactly the same upshot shown in Fig. 4. For the case of $P_{ss} = 45$ bar, the RO performance improves as ΔP^u increases from 20 to 40 bar. For example, Fig. 5 shows that the maximum achievable value of the permeate

Table 2
Effect of pulse width at optimal pulse amplitude

P_w	q/q_{ss}	C_p/C_{pss}	P_f	u_f
1	1.387	0.814	30	21.799
5	1.388	0.813	30	21.788
25	1.394	0.809	30	21.746
50	1.403	0.805	30	21.692
75	1.413	0.803	30	21.677
100	1.420	0.805	30	21.842
125	1.425	0.813	30	22.340
150	1.428	0.824	30	22.995
175	1.429	0.838	30	23.842
200	1.428	0.853	30	24.640
225	1.429	0.867	30	25.241
250	1.427	0.882	30	25.912
275	1.424	0.898	30	26.507
300	1.415	0.918	30	27.192

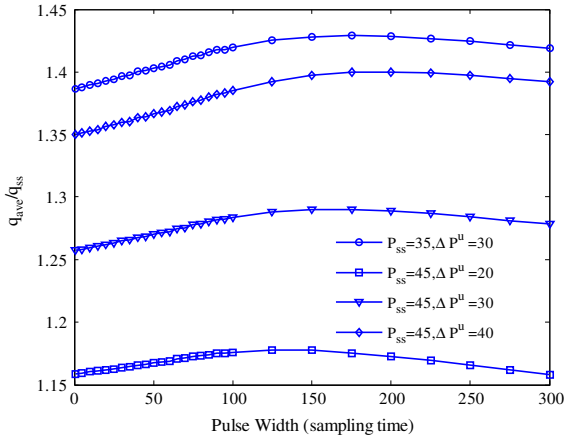

Fig. 5. The variation of the permeate flow with pulse width at different values for the upper limit on feed pressure.

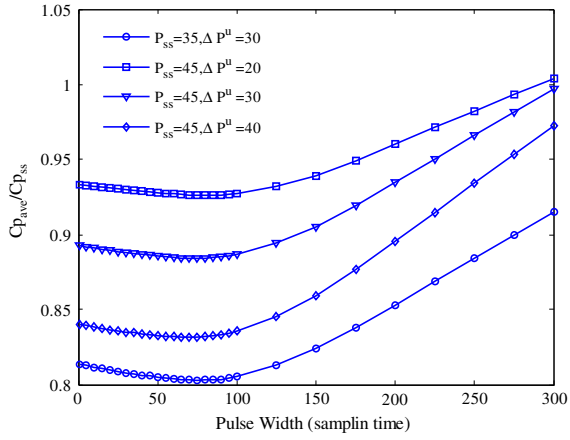

Fig. 6. The variation of the product salt concentration with pulse width at different values for the upper limit on feed pressure.

flow as a ratio to its steady-state value at $P_{ss} = 45$ bar can increase from 17% at $\Delta P^u = 20$ to 37% at $\Delta p^u = 40$ bar. Moreover, the optimum pulse width at which the maximum q_{ave}/q_{ss} occurs varies with Δp^u. Fig. 5 illustrates that the optimum P_w is around 150 for $\Delta p^u = 20$ bar and around 200 for $\Delta p^u = 40$ bar. Fig. 6 shows similar trend for the salt concentration with respect to the upper limit on the feed pressure. In fact, the salt concentration ratio (Cp_{ave}/Cp_{ss}) improves from 6% reduction at $\Delta P^u = 20$ bar up to 19% reduction at $\Delta P^u = 40$ bar. However, the pulse width effect on Cp_{ave}/Cp_{ss} is different than that on q_{ave}/q_{ss}. In this case, the optimum P_w is almost the same for all Δp^u which is around 70 sampling units. Furthermore, increasing P_w has an adverse impact on the salt removal as Fig. 6 demonstrates that the salt concentration ratio worsen rapidly as P_w grows.

On the other hand, Figs. 5 and 6 indicate that the results at smaller value for the initial value of the feed pressure (P_{ss}), that is, 35 bar outperforms that obtained at $P_{ss} = 45$ bar for all cases of Δp^u. However, it should be noted that the results at higher P_{ss} is referenced to the steady-state value of q and C_p which are obtained when the process is operated at steady-state value of $P_f = 45$ bar and $u_f = 38$ cm/s. Whereas the results at lower P_{ss} is referenced to the steady-state value of q and C_p that are obtained when the process is operated at steady-state mode of $P_f = 35$ bar and $u_f = 38$ cm/s. For reasonable comparison, all obtained curves in Figs. 5 and 6 are recalculated for q_{ss} and Cp_{ss} obtained at $P_f = 35$ bar. The new consequences are shown in Figs. 7 and 8. In due course, the effect of increasing Δp^u and P_w remain the same as before. For example, increasing Δp^u always improve the performance of

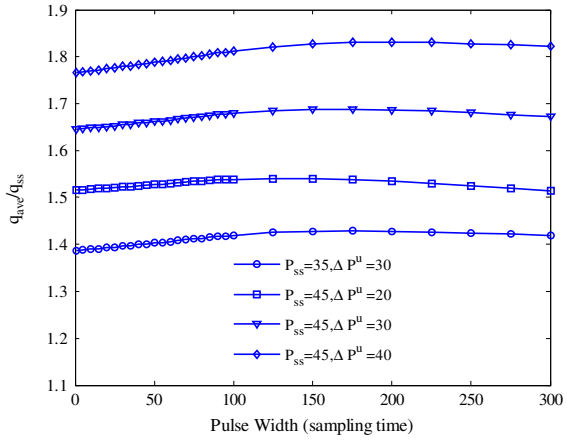

Fig. 7. The variation of the permeate flow with pulse width at different values for the upper limit on feed pressure based on $P_f = 30$ bar.

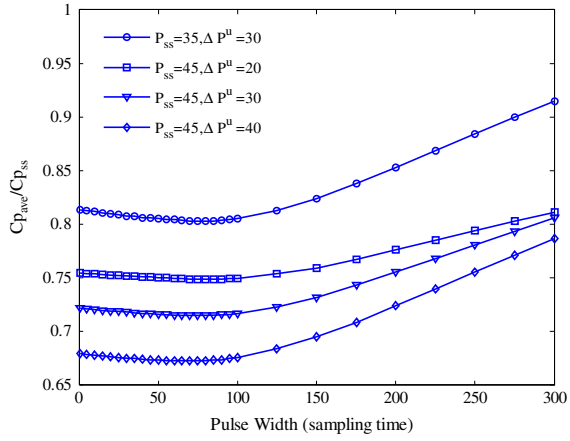

Fig. 8. The variation of the product salt concentration with pulse width at different values for the upper limit on feed pressure based on $P_f = 30$ bar.

q and C_p. Similarly, increasing P_w improves the permeate flow but decreases the salt removal. The only notable difference is that the RO performance at $P_{ss} = 35$ bar is no longer better than those obtained at $P_{ss} = 45$ bar. It can be concluded that higher value for P_{ss} allow operating at larger pressure oscillation magnitude increasing the chances to improved RO performance in terms of higher q_{ave}/q_{ss} and lower Cp_{ave}/Cp_{ss}.

For all cases above, the decrease in salt concentration at membrane wall, which was predicted by the model, is the reason for this improvement in permeation rate. Because the salt concentration is proportional to that at the wall, similar effect is observed. This agrees with the widely accepted argument that relates such enhancement to the decrease in concentration polarization Moreover, the trends obtained were consistent with the experimental results reported in the literature.

4. Conclusions

The performance of the periodic operation of a RO desalination unit using a validated dynamic model was investigated in this work. Symmetric cyclic variation of the feed pressure and velocity is imposed in the process dynamic operation. Rectangular pulses were used to simulate the cyclic input functions. The rectangular pulses are chosen for periodic forcing because they are more suitable for digital control applications. The characteristics of the pulses, such as pulse width and amplitude, are determined by numerical optimization tools. The results of the simulated periodic operation indicated performance improvement in terms of increased permeate production and decreased salt concentration in the product. For example, an enhancement up to 40% in the permeate production and to −20% in the salt concentration can be obtained. Moreover, it is found that the pulse amplitude and the central value of the periodic function play an important role in the amount of performance enhancement. Specifically, larger pulse amplitude of the feed pressure has a positive effect on the permeate flow increment and salt content reduction. Similar characteristic is observed for the effect of the mean value of the cyclic pulses. As far as the pulse period is concerned, there is a unique value of the pulse width at which maximum permeate production occurs and another unique value at which maximum salt reduction takes place. In fact, maximizing the permeate production requires a pulse width between 100 and 200 sampling units, while the minimizing the salt concentration requires pulse width between 50 and 100 sampling units.

The observed process enhancement when periodic operation is used is attributed to the reduction in the effect of concentration polarization that was successfully predicted by the model. In practice, frequent pulsation may not be preferable because it may affect the piping and fittings. Thus, the application may be suitable when large sampling time is used.

Acknowledgments

The Authors are thankful to the Deanship of Scientific Research at King Saud University (Research Group Project No: RGP-VPP-188) for the financial support of this research.

Nomenclature

A_{m1}, A_{m2}	pulse amplitude for input 1 and 2	atm, cm/s
$c_{b,i}$	salt concentration in brine in ith increment	mol/cm^3
c_F	salt concentration in the feed	mol/cm^3
$c_{p,i}$	salt concentration in permeate in ith increment	mol/cm^3
$\overline{C_p}$	average value for c_p	mol/cm^3
c_{pss}	steady-state value for cp	mol/cm^3
$c_{w,i}$	salt concentration at the wall in ith increment	mol/cm^3
D_s	diffusion coefficient of salt in solution	cm^2/s
d	internal diameter of tube	cm
F	feed flow rate	cm^3/s
f_F	fanning factor	—
$J_{v,i}$	volume flux density through membrane in ith increment	cm/s
j_i	Chilton–Colburn factor	—
L_p	hydraulic permeability	cm/s atm
$p_{b,i}$	brine pressure in ith increment	atm/m^2
P_f	feed pressure	atm/m^2
$p_{p,i}$	permeate pressure in increment i	atm/m^2
P_w	pulse width	Sample unit
q	permeate production rate	cm^3 /s
$\overline{q}$	average value for q	cm^3 /s
q_{ss}	steady state of q	cm^3/s
R	Universal gas constant	cm^3. atm/K. mol
R'_j	intrinsic salt rejection coefficient	—
Re	Reynolds number	—
Rr	recovery ratio	—
Sc	Schmidt number	—
T	operating temperature	°K
u_i	brine average velocity in ith increment	cm/s

U	input vector	—
u_f	feed velocity	cm/s
X	state vector	—
Δx	differential tube length	cm
w_1, w_2, w_3	weights on optimized variables	—

Greek

N	number of ions produced on complete dissociation of one molecule of electrolyte ($v=2$ in this work)	—
v_k	kinematic viscosity	cm^2/s
ρ_b	brine density	g/cm^3
ρ_p	permeate density	g/cm^3

Superscript

L	lower
U	upper

References

[1] S.M. Finnigan, J.A. Howell, The effect of pulsed flow on ultrafiltration fluxes in a baffled tubular membrane system, Desalination 79 (1990) 181–202.

[2] J.S. Vrouwenvelder, S.G.J. Heijman, X.D. Viallefont, D. van der Kooij, L.P. Wessels, Periodic air/water cleaning for control of biofouling in spiral wound membrane elements, J. Membr. Sci. 287 (2007) 94–101.

[3] J.S. Vrouwenvelder, J.A.M. van Paassen, L.P. Wessels, A.F. van Dam, S.M. Bakker, The membrane fouling simulator: A practical tool for fouling prediction and control, J. Membr. Sci. 281 (2006) 316–324.

[4] N.M. Al-Bastaki, A. Abbas, Periodic operation of a reverse osmosis water desalination unit, Sep. Sci. Technol. 33 (1998) 2531–2540.

[5] T.J. Kennedy, R.L. Merson, B.L. McCoy, Improving permeation flux by pulsed reverse osmosis, Chem. Eng. Sci. 29 (1973) 1927–1931.

[6] S. Ilias, R. Govind, Potential applications of pulsed flow for minimizing concentration polarization in ultrafiltration, Sep. Sci. Technol. 25 (1990) 1307–1324.

[7] N.M. Al-Bastaki, A. Abbas, Improving the permeate flux by unsteady operation of a RO desalination unit, Desalination 123 (1990) 173–176.

[8] A. Abbas, N.M. Al-Bastaki, Flux enhancement of RO desalination process, Desalination 132 (2000) 21–27.

[9] A.A. Abufayad, Performance characteristics of a cyclically operated seawater, desalination plant in Tajoura, Libya, Desalination 156 (2003) 59–65.

[10] N.M. Al-Bastaki, A. Abbas, Use of fluid instabilities to enhance membrane performance: A review, Desalination 136 (2001) 255–265.

[11] M. Al-haj Ali, A. Ajbar, E. Ali, K. Alhumaizi, Study of cyclic operation of RO desalination process, Can. J. Chem. Eng. 89 (2010) 299–303.

[12] M. Al-haj Ali, A. Ajabr, E. Ali, K. Alhumaizi, Modeling the transient behavior of an experimental reverse osmosis tubular membrane, Desalination 245 (2009) 194–204.

[13] J.M. Douglas, Process Dynamics and Control, Prentice-Hall, Englewood Cliffs, NJ, 1972.

[14] F.L. Harris, G.B. Humphreys, K.S. Spiegler, Reverse osmosis (hyperfiltration) in water desalination, In: P. Meares (Ed.), Membrane Separation Processes, Elsevier Scientific, New York, NY, pp. 121–187, 1976.

Appendix A Dynamic Model of the RO Unit

The model assumptions and the detailed derivation of model equations can be found in [12], In this Appendix, the model is briefly presented.

The membrane module is divided into n increments, and mass and energy balances are made for each segment. The permeate flux ($J_{v,i}$) through the membrane at, increment i, is described by the three parameter nonlinear Spiegler–Kedem (SK) model:

$$J_{v,i} = L_p[(p_{b,i} - p_{p,i}) - (R'_j)^2 vRTc_{w,i}] \tag{A.1}$$

where $p_{b,i}$ and $p_{p,i}$ are brine-side and permeate-side pressures, respectively, R'_j is the intrinsic salt rejection, and R is the ideal gas constant. c_{wi} is the wall brine concentration at the ith increment, it is calculated using the flowing equation:

$$c_{w,i} = c_{b,i} \times \frac{\exp\left(\frac{J_{v,i}\times Sc^{2/3}}{j_i \times u_i}\right)}{R'_j + (1 - R'_j) \times \exp\left(\frac{J_{v,i}\times Sc^{1/3}}{j_i \times u_i}\right)} \tag{A.2}$$

with Sc is Schmidt number and j_i is Chilton–Colburn factor. For turbulent flow in smooth circular tubes, it is given by [14]:

$$j_i \cong 0.0395 \mathrm{Re}_i^{-1/4} \tag{A.3}$$

with Re_i being the local Reynolds number in ith increment.

The dynamics of salt concentration in the brine leaving increment i are given by the following equation

$$\frac{dc_{b,i+1}}{dt} = \left(\frac{u_i \times c_{b,i}}{\Delta x}\right) - \left(\frac{u_{i+1} \times c_{b,i+1}}{\Delta x}\right) - \left((1 - R'_j) \times \frac{4J_{v,i}}{d}\right) \times c_{w,i} \tag{A.4}$$

Here, u_{i+1} is the velocity of brine leaving the ith increment. It can be obtained from a volumetric balance about the ith increment and is given by

$$u_{i+1} = u_i - 4J_{v,i}\Delta x/d \tag{A.5}$$

with Δx and d being the increment length and tube diameter, respectively.

The energy balance for the ith increment is used to calculate the pressure in the brine-side for different ith increments. It can be proved that the pressure leaving the t-th increment can be calculated as follows:

$$p_{b,i+1} = \left(\frac{u_i}{u_{i+1}}\right) \times \left(p_{b,i} + 0.5 \times 10^{-7} \times \rho_{b,i} \times u_i^2 - 2 \times 10^{-7} \times f_F \times \Delta x \times u_i^2 \times \frac{\rho_{b,i}}{d}\right) - \left(\frac{4\Delta x \times J_{v,i}}{d \times u_{i+1}}\right) \times \left(p_{b,i} + 0.5 \times 10^{-7} \times \rho_{p,i} \times J_{v,i}^2\right) - 0.5 \times 10^{-7} \times \rho_{b,i} \times u_{i+1}^2 \Delta p_{b,i} = p_{b,i+1} - p_{b,i} \tag{A.6}$$

with ρ_{bi} and ρ_{pi} being the brine and permeate density, respectively, and f_F is Fanning friction factor given by

$$f_F \cong 2 \times j \tag{A.7}$$

The permeate production rate for the ith increment is given by

$$q_i = J_{v,i} \times \pi \times d \times \Delta x \tag{A.8}$$

The cumulative production rate from all increments is

$$q = \sum_{i=1}^{n} J_{vi} \times \pi \times d \times \Delta x \tag{A.9}$$

The cumulative average salt concentration of the product water can be obtained by multiplying the quantity of water produced in certain increment by the salt concentration in that increment. Rearranging the resulted equation gives

$$c_{p,i} = c_{p,i-1} \times \frac{\sum_{i=1}^{n-1} q_i}{q} + \frac{(1 - R'_j) \times c_{w,i} \times J_{v,i} \times \pi \times d \times \Delta x}{q} \tag{A.10}$$

When cyclic mode of operation is used, the ratio of the unsteady state to steady flow mass transfer coefficients was approximated by [11]:

$$\frac{k_p}{k_s} = 0.5 \times |1 + \frac{u_p}{u_s}|^n + 0.5 \times |1 - \frac{u_p}{u_s}|^n \tag{A.11}$$

with subscripts p and s referring to periodic and steady-state operations, respectively. u_p is the periodic velocity. $n = 1/3$ for laminar flow and $n = 0.8$ for fully developed turbulent flow.